Copyright ⓒ 2025 KSII

TDOA-MCM: A TDOA-based Multi-path Communication Mechanism for UWB Indoor Positioning

Xuan Lu[1,2], Jinhong Guo[1], Furong Peng[3*], and Yu Dong[4]
[1] College of Physics and Electronic Engineering, Shanxi University
Taiyuan 030006, P.R. China
[e-mail: xuanlu@sxu.edu.cn]
[2] Shanxi Key Laboratory of Wireless Communication and Detection, Shanxi University
Taiyuan 030006, P.R. China
[3] Institute of Big Data Science and Industry, Shanxi University
Taiyuan 030006, P.R. China
[e-mail: pengfr@sxu.edu.cn]
[4] College of Computer Science and Electronic Engineering, Hunan University
Changsha 410000, P.R. China
[e-mail: yudongltg@hnu.edu.cn]
[*]Corresponding author: Furong Peng

Received September 29, 2024; revised December 2, 2024; accepted January 8, 2025; published January 31, 2025

Abstract

UWB-based indoor positioning technique presents superior performance but suffers from accuracy degradation caused by clock desynchronization in real situations. This paper proposes a TDOA-based multi-path communication mechanism (TDOA-MCM) to address this issue. One base station transmits the signal that arrives at the tag via two paths. One is the direct path, and the other is via a relay station. According to the time difference between the two signals, the tag calculates its position using the Gaussian-Newton algorithm. The Cramer-Rao bound is used to evaluate the performance of the proposed TDOA-MCM. Due to an additional path from the transmitter to the relay, its performance is slightly worse than the ideal clock-synchronized TDOA which is not achievable in real situations. However, it outperforms the TDOA with clock drift or desynchronization, which is validated by simulation results. Using DW1000-based commercial positioning modules, single and multiple tag positioning experiments were conducted, achieving positioning errors of less than 10 cm.

Keywords: UWB, Indoor positioning, TDOA positioning, multi-path communication, clock synchronization.

1. Introduction

The Internet of Things (IoT) is significantly changing people's way of life, bringing many smart and convenient services [1]. Location information for personnel or items plays an important role in intelligent services. For example in a restaurant's robot delivery system, robots rely on real-time location to compute the route from the kitchen to the customer's table. When multiple robots operate in the same environment, location information helps coordinate their actions to prevent collisions and interference. In such an indoor restaurant environment, global navigation satellite systems like Global Positioning System (GPS) and Beidou cannot provide precise positioning due to signal attenuation [2]. Signals are significantly weakened or blocked by walls, ceilings, and other structural elements of buildings, and multi-path interference also leads to inaccuracies. Besides, indoor environments cannot reach a clear line of sight to multiple satellites. The signals are too weak in basements, tunnels, or mines, to use satellite systems. Because of these limitations, alternative indoor positioning technologies, such as Ultra-wideband (UWB) are used to provide the high accuracy and reliability needed for indoor applications [3][4]. Compared to other indoor positioning technologies, UWB mainly offers the following advantages [5][6][7].

- High precision: UWB offers centimeter-level accuracy for positioning, which is significantly higher than the meter-level accuracy provided by Bluetooth, Radio-Frequency Identification (RFID), and Wi-Fi.
- High data rate: UWB supports higher data transfer rates than RFID, making it suitable for applications that require fast and efficient data exchange.
- Low interference: UWB operates over a GHz-level frequency range, which reduces the likelihood of interference with other wireless technologies. This ensures more reliable communication and positioning in environments with multiple wireless systems.
- Low power consumption: UWB is designed to consume less power than WiFi, which is more suitable for battery-operated devices and applications where energy efficiency is critical.
- Secure communication: Its wide spectrum and low power spectral density make it more difficult to detect and intercept, offering better security for sensitive data transmission than other wireless technologies.

Similar to satellite positioning, the UWB system also sets up several base stations indoors, where these base stations communicate with the tags to be located. Various UWB-based positioning methods have been proposed based on their communication mechanisms.

- Angle of Arrival (AOA) [8]. The signal transmitted by the base station is received by an array of antennas at the receiving device (tag). The difference in arrival times of the signal at each antenna in the array is measured and used to calculate the angle of the signal's arrival, i.e., the base station. Since the locations of the multiple base stations are known during setup, the tag's position can be located. However, in indoor environments, signals often reflect off surfaces, causing multi-path interference, which can create errors in the angle calculation. It also requires complex antenna arrays, increasing the cost and difficulty of implementation in practical applications.
- Received Signal Strength Indication (RSSI) [9][10]. In the RSSI mechanism, the tag measures the signal strength from multiple base stations. Generally, it assumes that stronger signals indicate closer proximity, while weaker signals suggest the tag is farther away. Then the distance between the receiver and each transmitter is estimated. By knowing the locations of the base stations, the tag is positioned by

triangulation/trilateration. RSSI is simple to implement, but its estimation is extremely sensitive to the signal transmission environment, and the positioning accuracy of RSSI is often unsatisfactory [11].

- Time of Arrival (TOA) [12]. TOA is based on distance measurement and triangulation/trilateration as well. The difference is that the tag measures the time it takes from transmitting to receiving, and the distance is calculated by multiplying the travel time by the signal's speed. However, this method relies on precise clock synchronization between the base stations and tags to ensure accurate distance measurements, which is a significant challenge in engineering applications [13].
- Two-Way Ranging (TWR) [14]. TWR determines the distance by measuring the round-trip time of a signal. When the tag receives the signal from the base station, it immediately sends a response back to the base. The signal's time of flight (TOF) is calculated by subtracting the signal processing time at the tag from the total time. This mechanism only requires relative time measurement instead of precise time synchronization between devices, and it is relatively simple to implement. However, errors can occur if the processing time at the tag is not accurately accounted for, and continuous sending and receiving of signals may increase power consumption.
- Time Difference of Arrival (TDOA) [15]. TDOA is a method that measures the difference in arrival times of the signal at multiple, spatially separated receivers. Usually, the signal is emitted from the tag at an unknown location and received by base stations at known positions. Each base station records the exact time the signal arrives. Since the receivers are synchronized, they can measure the time difference between when the signal arrives at each base station. Then the time differences are used to calculate hyperbolic curves. Each pair of base stations defines a hyperbola on which the tag must lie. The intersection of multiple hyperbolas determines the position of the signal source, i.e., the tag. Calculating the relative time differences of signal arrival, TDOA eliminates clock drift and desynchronization of TOA. Although the cost and complexity of the system increase compared to TOA, it often provides better accuracy in environments with multi-path effects. Nevertheless, it still requires synchronization among the base stations, which is difficult to implement in engineering applications.

2. Related Work

Clock synchronization is crucial in TDOA positioning accuracy, and many works have addressed this issue. The elliptical A-TDOA positioning system uses the "receive and retransmit" strategy to achieve high accuracy [16][17]. The process begins when the positioning device sends out a UWB pulse, which is amplified and retransmitted after reaching the target. The receiver captures signals from both the positioning device and the target, eliminating the need for a synchronization mechanism. This avoids the issue of clock offset, but the system's complexity is high, and the update rate is relatively low. The time-difference positioning method proposed by Whistle [18] achieves high precision through double signal detection and sampling counting techniques. Reference [19] and [20] increase reference nodes to improve positioning accuracy. In Reference [19], researchers propose an async-TDOA positioning model based on the principle of asynchronous time difference of arrival to determine the target position. However, this model requires the reference node to send positioning signals periodically, making it difficult to ensure that the tag sends the signal between two signal transmissions of the reference node. Reference [20] proposes a differential

UWB positioning method, which involves comparing and processing signals received by multiple receivers, significantly increasing the computational complexity during positioning. In Reference [21], a reference-free asynchronous UWB-TDOA ranging method is designed to improve positioning accuracy, but the communication process is too complex. Reference [22] proposes a P-TDOA method that uses a polynomial model to describe the nonlinear and time-varying TDOA measurements, providing instantaneous TDOA estimates. However, the P-TDOA method requires data from multiple frames to estimate TDOA, which affects the real-time performance of the algorithm and results in high computational complexity. Reference [23] presents a high-precision joint TDOA and FDOA positioning system. Although this method can improve positioning accuracy, the system's hardware and software design are relatively complex, and its computational complexity is high, making it highly dependent on hardware performance. Reference [24] utilizes artificial neural networks to estimate the TDOA to improve ranging accuracy. However, this method is limited by training data, has poor interpretability, and relies heavily on the computational power of servers.

This paper provides a TDOA-based multi-path communication mechanism, TDOA-MCM, that does not require clock synchronization or extra devices for clock calibration. The communication mechanism is simple, cost-effective, easy to deploy, and offers positioning accuracy comparable to traditional TDOA methods. The positioning performance is evaluated using the Cramer-Rao lower bound. Simulations and indoor experiments validate the theoretical analysis.

Focusing on clock synchronization issues, this study did not consider non-line-of-sight propagation or noise interference [25][26], although they are also important for positioning accuracy.

3. TDOA-based Multi-path Communication Mechanism

3.1 Principle of the basic TDOA

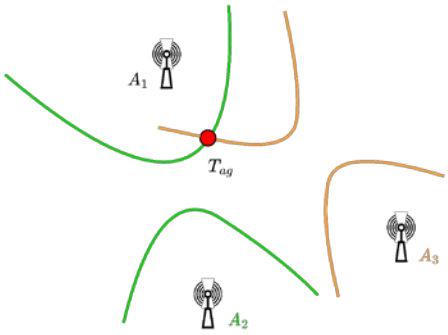


Fig. 1. Geometric diagram of the two-dimensional TDOA positioning on a plane.

Fig. 1 shows the geometric diagram of the two-dimensional TDOA positioning on a plan [21]. Assume that the base stations are clock-synchronized, with known coordinates of $A_i(x_i, y_i)$, $i = 1,2,3$, and the tag is at an unknown position $T_{ag}(x, y)$. If the tag sends a signal at time zero, the base stations will receive it at time t_{Ti}, respectively. Then the tag should be on a hyperbola with A_i and A_j as foci and a constant distance difference of $c \cdot (t_{Ti} - t_{Tj})$ [27], i.e.,

$$\|T_{ag} - A_i\| - \|T_{ag} - A_j\| = c \cdot \left(t_{T_i} - t_{T_j}\right), i \neq j \tag{1}$$

where $\|\cdot\|$ calculates the Euclidean distance, c is the speed of electromagnetic wave propagation, $3 \times 10^8 m/s$, and the subscript $i \neq j$ means A_i and A_j are two different base stations. As on a plane, two sets of such hyperbolas can determine the tag's position, and at least three base stations are required. However, solving the tag's position can result in significant deviations when the base station clocks are not synchronized exactly in a real situation. Increasing the number of base stations is a common choice to improve positioning accuracy, but it cannot solve the problem fundamentally.

3.2 Principle of the TDOA-MCM

To address the clock synchronization issue, we propose a TDOA-based communication mechanism that involves multi-path propagation as illustrated in **Fig. 2**. It consists of a transmitter base station A_1, several relay base stations $A_i, i = 1,2,3$, and the tag T_{ag} to be located. After a signal is emitted by A_1, the tag receives it and records the moment it arrives. The relays operate the same way and forward the signal immediately after receiving it. Basically, the direct path from the transmitter A_1 to the tag and the multi-paths via the relay station form a triangle. Since the sum of any two sides of a triangle must be greater than the third side, the signal from A_1 on the direct path always arrives earlier than the forwarded signal on the multi-path.

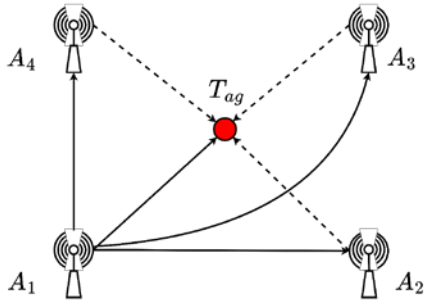


Fig. 2. Geometric Path of Signal Transmission in TDOA-MCM.

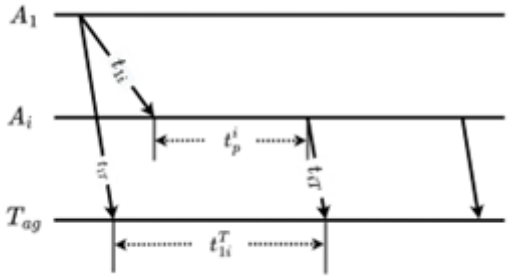


Fig. 3. Timing diagram of signal transmission in TDOA-MCM.

To illustrate this process in detail, **Fig. 3** shows the timing diagram of the signal transmission, in which t_{1i} and t_{1T} represent the flight time of the signal from the transmitter A_1 to the relay A_i and the tag T_{ag}, respectively. t_{iT} represents the flight time of the forwarded signal from A_i to T_{ag}. Then, we can get $\|A_i - A_1\| = c \cdot t_{1i}$, $\|T_{ag} - A_i\| = c \cdot t_{iT}$, and $\|T_{ag} - A_1\| = c \cdot t_{1T}$. But note that their clocks are not supposed to be exactly synchronized. As all the time is based on their local clocks, the time difference between sending and receiving that we obtain is not the accurate flight time but includes clock errors. It means we cannot know the exact distances of direct or indirect paths. However, we can get the distance difference, as the subtraction will

offset the clock errors of the two paths.

$$\delta d_{1i} = \|A_i - A_1\| + \|T_{ag} - A_i\| - \|T_{ag} - A_1\| = c \cdot \left(t_{1i}^T - t_p^i\right) \tag{2}$$

where t_p^i the time that relay A_i forwards the signal, which is easy to get if the signal is forwarded twice. The first time is for the start time of the forwarding process, while the second time is for the end time. t_{1i}^T represents the time between the tag receiving the signal from A_1 and the tag receiving the signal from A_i.

In equation (2), only the tag's coordinates T_{ag} are unknown variables, and they can be solved if the number of base stations is sufficient in the positioning system. For example, the number is three for a two-dimensional positioning on a plane.

Using the distance difference to solve the tag's coordinates eliminates the need for clock synchronizations. However, in a real positioning system, the errors are mainly caused by the placement of the devices, the hardware factors, and environment noise, which cannot be ignored. The first two factors result in constant errors, and the environment noise follows a Gaussian distribution [28].

Assuming the Gaussian error $n_i \sim N\left(0, \sigma_i^2\right)$, equation (2) becomes a system of Diophantine equation (3), and the Gauss-Newton method, a nonlinear iterative algorithm, is used to solve the problem.

$$\|A_i - A_1\| + \|T_{ag} - A_i\| - \|T_{ag} - A_1\| + n_i = c \cdot \left(t_{1i}^T - t_p^i\right) \tag{3}$$

Moving terms involving T_{ag} to one side and let $c \cdot \left(t_{1i}^T - t_p^i\right) - |A_i - A_1| = r_{1iT}$, equation (3) is simplified to

$$\|T_{ag} - A_i\| - \|T_{ag} - A_1\| + n_i = r_{1iT} \tag{4}$$

The solution is considered optimal when the sum of squared residuals in equation (5) is minimized.

$$T_{ag} = \arg\min_x \left[\sum_i \left(r_{1iT} - \|T_{ag} - A_i\| + \|T_{ag} - A_1\|\right)^2\right] \tag{5}$$

It requires an appropriate initial value and then iterates to approximate the global optimal solution. According to Reference [29], the k-th iteration is calculated as equation (6),

$$T_{ag}^{k+1} = T_{ag}^k - \boldsymbol{W}^k\left(r_i - \|T_{ag}^k - A_i\| + \|T_{ag}^k - A_1\|\right) \tag{6}$$

where $\boldsymbol{W}^k = \left(\boldsymbol{H}_k^T \boldsymbol{H}_k\right)^{-1} \boldsymbol{H}_k^T$, $\boldsymbol{H}_k = \frac{\partial\left(\|T_{ag}^k - A_i\| - \|T_{ag}^k - A_1\|\right)}{\partial T_{ag}}$ and $\boldsymbol{H}$ is the Jacobian matrix.

Note that the tag does not emit signals throughout the process, which is so-called "passive". Theoretically, if there are multiple tags in the positioning system, they can operate independently without affecting each other. Another advantage of the passive mechanism is its invisibility which protects the privacy of tag users.

3.3 Performance of the TDOA-MCM

To verify the TDOA-MCM proposed in this paper, the Cramer-Rao Lower Bound (CRLB) is cited as a metric to evaluate the positioning accuracy of T_{ag}. CRLB is the lower bound of the variance of unbiased parameter estimates [16], here, written as

$$var\left(T_{ag}\right) \geq \text{CRLB} = G\left(T_{ag}\right)^{-1} \tag{7}$$

where $G(\cdot)$ is the Fisher information matrix.

In the positioning scenario, the coordinates of the T_{ag} are determined by the distance measurements between base stations and the tag, in which the main error arises. Since the environmental noise follows a Gaussian distribution, the distance measurement vector r follows a Gaussian distribution as well. Denote $r \sim N(\boldsymbol{R}, \boldsymbol{Q})$, and the Fisher information

matrix can be written as equation (8) [30].

$$G(T_{ag}) = \left(\frac{\partial \boldsymbol{R}}{\partial T_{ag}}\right) \boldsymbol{Q}^{-1} \left(\frac{\partial \boldsymbol{R}}{\partial T_{ag}}\right)^{T} \tag{8}$$

where $\boldsymbol{R}$ is the mean of the measurement vector and $\boldsymbol{Q}$ is the covariance matrix of error.

Denote r_{ij} as the distance measurement between device i and j, and T is the subscript for the tag. For a typical two-dimensional TDOA positioning in **Fig. 1**, r_{T1}, r_{T2}, r_{T3} should be measured to obtain the distance difference vector $r_{TDOA} = [r_{T1} - r_{T2}, r_{T1} - r_{T3}]^T$. Obviously, r_{TDOA} follows a Gaussian distribution $N(\boldsymbol{R}_{TDOA}, \boldsymbol{Q}_{TDOA})$, where $\boldsymbol{R}_{TDOA}$ is the mean of the vector $[r_{T1} - r_{T2}, r_{T1} - r_{T3}]^T$ and $\boldsymbol{Q}_{TDOA} = \text{diag}[\sigma^2_{r_{T1}-r_{T2}} - \sigma^2_{r_{T1}-r_{T3}}]$. $\sigma^2_{r_{T1}-r_{T2}}$ and $\sigma^2_{r_{T1}-r_{T3}}$ are the covariance of $r_{T1} - r_{T2}$ and $r_{T1} - r_{T3}$, respectively. For the TDOA-MCM proposed in this paper, the distance difference vector $r_{MCM} = [r_{12} + r_{2T} - r_{1T}, r_{13} + r_{3T} - r_{1T}]^T$, follows a Gaussian distribution $N(\boldsymbol{R}_{MCM}, \boldsymbol{Q}_{MCM})$.

$$\boldsymbol{R}_{MCM} = -\boldsymbol{R}_{TDOA} + [r_{12}, r_{13}]^T \tag{9}$$

$$\frac{\partial \boldsymbol{R}_{MCM}}{\partial T_{ag}} = -\frac{\partial \boldsymbol{R}_{TDOA}}{\partial T_{ag}} + \frac{\partial [r_{12}, r_{13}]^T}{\partial T_{ag}} \tag{10}$$

$$\boldsymbol{Q}_{MCM} = \boldsymbol{Q}_{TDOA} + diag[\sigma^2_{12}, \sigma^2_{13}] \tag{11}$$

where $\sigma^2_{12}, \sigma^2_{13}$ are the covariance of the measured r_{12} and r_{13}, respectively.

Observing equations (9)-(11), the proposed TDOA-MCM has additional terms about r_{12} and r_{13} compared to the ideal clock-synchronized TDOA. This is because the TDOA-MCM positioning mechanism has an additional path from A_1 to A_i. The terms appear to have deteriorated the positioning performance, but considering that the path is irrelevant to the tag, the impact of the terms is slight. Besides, the ideal clock synchronization in TDOA is not achievable in real situations. Each additional communication for clock compensation or calibration will aggravate the effects of noise.

4. Experimentation

This section presents MATLAB simulations and indoor experiments to demonstrate that the proposed TDOA-MCM is insensitive to clock desynchronization by discussing positioning errors in detail.

4.1 Simulation

Set four base stations located at the vertices of a rectangle with coordinates (0, 0), (0, 10), (10, 10), and (10, 0) with the unit in meters, respectively. Five positioning points are uniformly distributed in the rectangular area surrounded by the four base stations, which are top left (2.5, 7.5), top right (7.5, 7.5), bottom left (2.5, 2.5), bottom right (7.5, 2.5), and middle (5, 5). Gaussian noise with an average value of 0 and a standard deviation of 0.01 was added to simulate environment noise in all simulations. Each point is located 1000 times by ideal TDOA, TDOA with clock desynchronization, and TDOA-MCM. The clock desynchronization consists of a fixed clock difference and a random clock drift. Using the Tag's clock as a reference, the fixed clock differences of the four base stations are +1 ns, +0.5 ns, -1 ns, and -0.5 ns, respectively, and the random clock drift ranges from 0 to 1 ns. Simulation results are shown in **Fig. 4**.

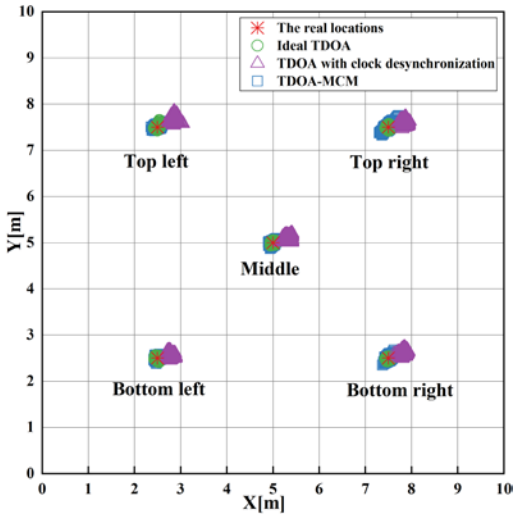
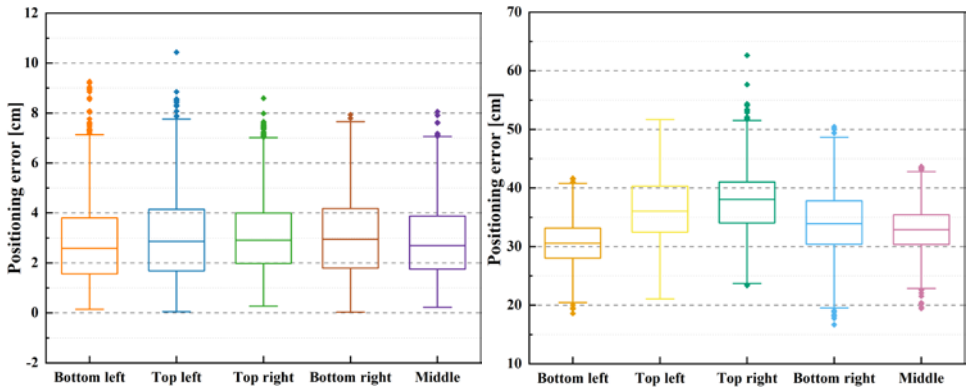


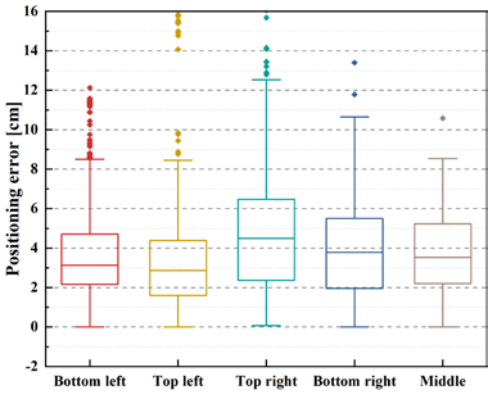
Fig. 4. Simulation results for the ideal TDOA, TDOA with desynchronization, and the proposed TDOA-MCM.

The positioning results are all close to the real locations. The errors of ideal TDOA are minimal, and the results of the TDOA with desynchronization have a relatively consistent offset due to the fixed clock differences between base stations and the Tag. Specifically, all errors are statistically represented in **Fig. 5**, displaying errors of five points, respectively, in the box-and-whisker plot. The box represents the interquartile range, which covers the data from the first quartile (Q1, 25% of the error falls below this point) to the third quartile (Q3, 75% of the error falls below this point), i.e., the box contains the middle 50% of the data. The middle line in the box (Q2) represents the median of all the errors. The results show that:

As expected, the accuracy of the ideal TDOA is the highest, as it assumes the clocks are fully synchronized and the amount of communication is minimal. All the errors are below 7.7 cm, and the median errors are 2.5 cm, 2.8 cm, 2.9 cm, 2.9 cm, and 2.6 cm, respectively. However, it is impossible to achieve in real situations.



(a) Ideal TDOA (b) TDOA with clock desynchronization



(c) Simulation errors displayed in box-and-whisker plots

Fig. 5. Simulation errors displayed in box-and-whisker plots.

When clock desynchronization is added to the ideal TDOA, the positioning errors increase significantly. Most of the data in the box is distributed between 30 and 40 cm, with a maximum value of 51.7 cm. The median errors are 30.5 cm, 36 cm, 38 cm, 33.8 cm, and 32.2 cm, respectively, quite larger than the ideal TDOA.

The proposed TDOA-MCM also involves fixed clock difference and clock drift. The errors are all below 12.5 cm, with Q3 below 6.4 cm. The median errors are 3.1 cm, 2.8 cm, 4.5 cm, 3.7 cm, and 3.5 cm, respectively. Its performance is slightly worse than the ideal TDOA because of the additional path, but it is much better than TDOA with clock desynchronization. The simulation results are consistent with the CRLB calculated in Subsection 2.3.

4.2 Indoor experiments

UWBMini3s shown in **Fig. 6** are used as base stations and tags for indoor positioning experiments. It's a DW1000-based commercial positioning module, controlled by an STM32F103T8U6 processor. DW1000 is a radio frequency (RF) chip that receives and forwards information frames.

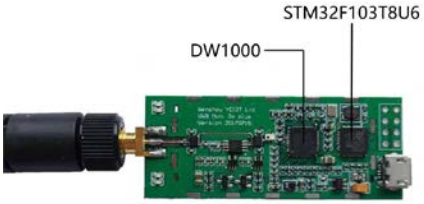


Fig. 6. Positioning module, UWBMini3s.

4.2.1 Single tag positioning

As shown in **Fig. 7**, three modules were arranged in a classroom of 6×8 m^2 to send and relay positioning signals as base stations. Another module was set as the tag node to receive the signals without relaying them, achieving passive positioning. All the modules were located at the same height, 1.8m, to ensure they were on a plane.



Fig. 7. Scenario of the single tag positioning.

Three base stations were set at (0, 0), (6, 0), and (0, 8), and the tag node was moved to five places Without loss of generality: upper left (1, 6), upper right (5, 6), lower right (5, 2), lower left (1, 2), and center (3, 4) in meters. Each location was measured 2500 times. The positioning results are visualized in **Fig. 8**, where the star markers represent the actual reference point locations, and the dots indicate the positioning points obtained through the multi-path positioning method.

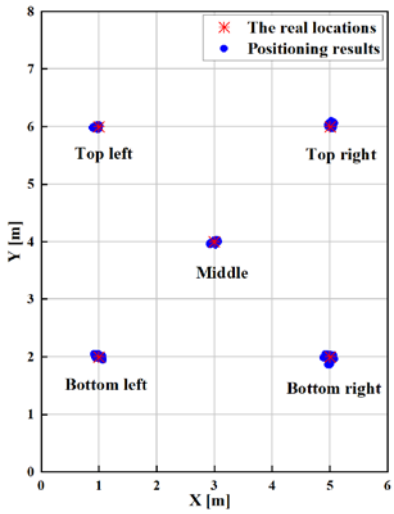


Fig. 8. TDOA-MCM positioning results of the single tag.

It can be observed that the positioning results are very close to the real locations of the tags, indicating good positioning performance. Again, the errors are statistically represented in a box plot of **Fig. 9**. All the errors of the five points are less than 10 cm except for some bad points, and most of the deviations are converged within the range of 2 cm to 6 cm. This demonstrates that multi-path positioning achieves high accuracy in practical positioning tasks. Furthermore, the compact shape of the box plot suggests that the errors are not highly dispersed, further confirming the stability and reliability of the multi-path positioning method.

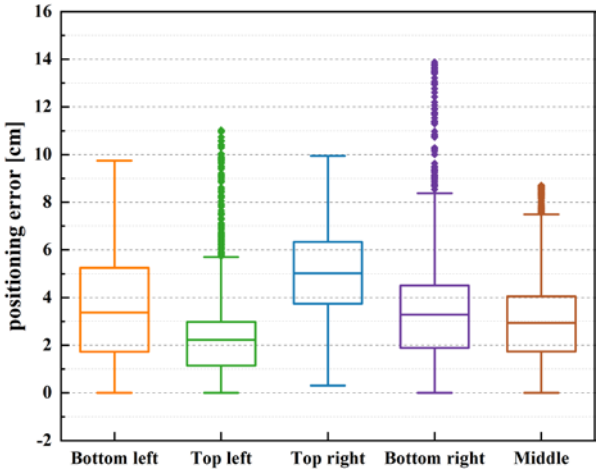


Fig. 9. Box plot of the positioning errors.

As in the real situation, the positioning error is mainly caused by the placement of the devices, the hardware factors, and environment noise, in which the first two factors result in a constant error, and the environment noise follows a Gaussian distribution [25]. The constant error can be compensated, and the Gaussian distribution of environment noise is the main source of the uncertainty in the positioning process. Fortunately, it can be suppressed by Gaussian filtering. **Fig. 10** shows 3000 points of raw data, where we can see the errors greatly converged after filtering. Theoretically, the errors will converge to a straight line, but in the real situation, there are still some fluctuations, which may be caused by temperature changes and clock drift of the chip itself [31][32].

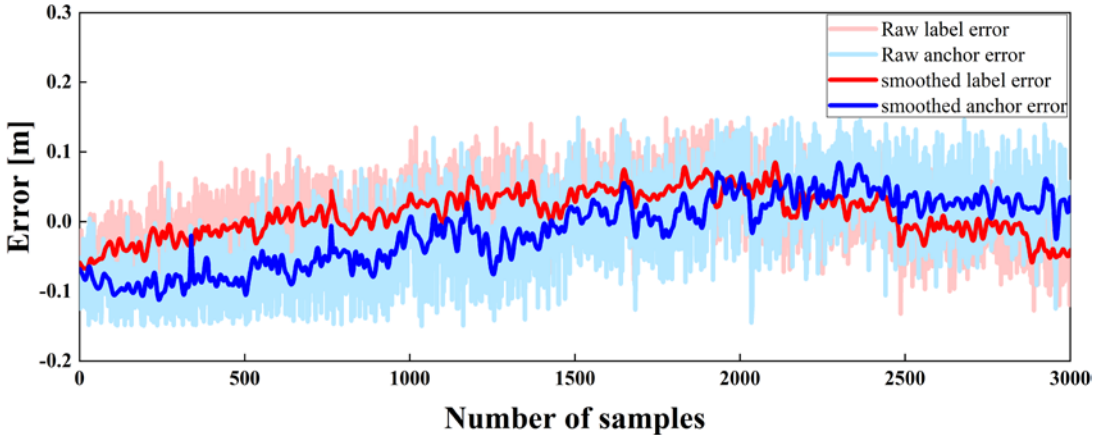


Fig. 10. Gaussian filtering to environment noise.

4.2.2 Multiple tag positioning

To validate the capability of multi-tag positioning of the proposed TDOA-MCM, another two tags were added based on Single tag positioning, and the three tags were tested simultaneously as shown in **Fig. 11**. Their coordinates are set as Tag1 (3, 4), Tag2 (1, 2), and Tag3 (5, 2), respectively. Using a multi-path positioning algorithm, the positioning results of 5000 continuous measurements are visualized in **Fig. 12** and their errors are statistically in **Fig. 13**.

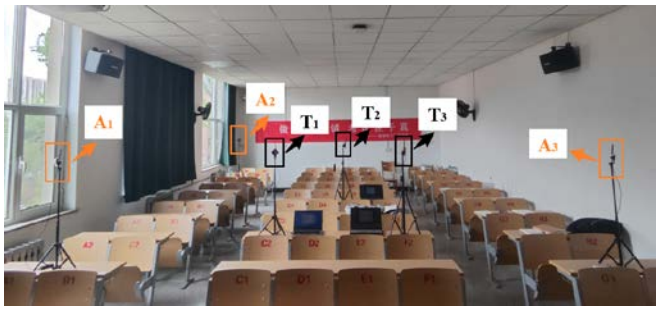


Fig. 11. Scenario of the three tags operating simultaneously.

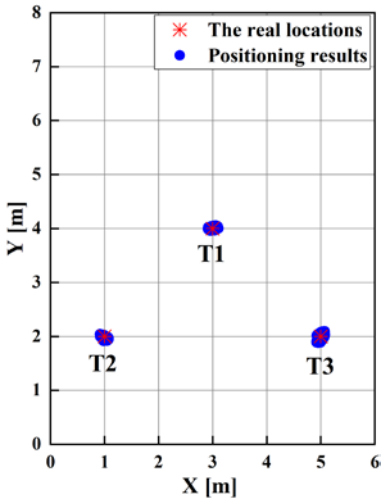


Fig. 12. Positioning results of the three tags operating simultaneously.

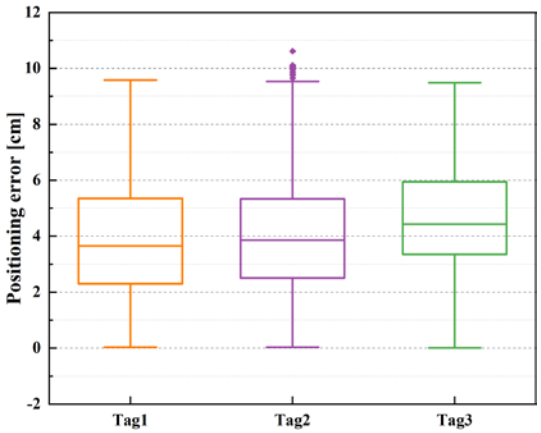


Fig. 13. Errors of the three tags operating simultaneously.

When the number of tags increases to three, the multi-path positioning system still keeps its performance. The errors are converged between 2 cm and 6 cm, with the means of 3.656 cm, 3.864 cm, and 4.2 cm, respectively, and a maximum of less than 10 cm except for some bad points. Besides, **Fig. 14** shows the cumulative distribution function of the root mean square errors (RMSE) for the three tags, where x represents the RMSE values, measured in meters, and $F(x)$ represents the cumulative probability of RMSE being less than or equal to x. The

curves present a similar trend for the three tags, indicating similar performances of different tags. The difference between the curves is basically a constant in the main section and can be attributed to tag locations. This demonstrates that the multi-path positioning method can handle multiple tags simultaneously while maintaining high positioning accuracy and good stability in real positioning scenarios, and makes it suitable for multiple terminals or heavy load conditions such as staff/stuff tracking within hospitals, factories, or underground mines.

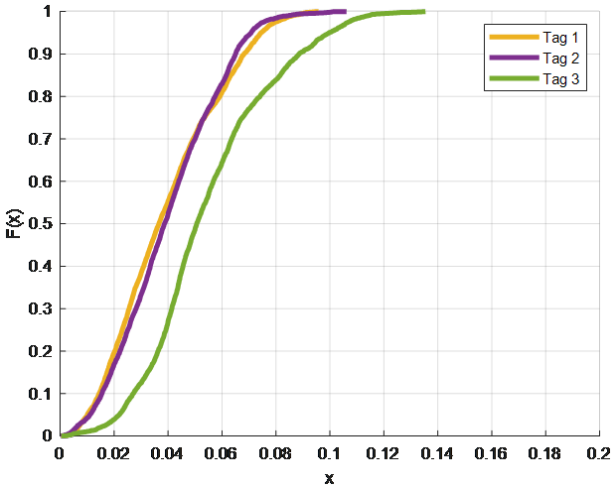


Fig. 14. Probability density distribution of the errors.

Table 1 presents a comparison with other TDOA-based positioning methods, including their experimental setup, clock synchronization, complexity, and positioning errors. Note that the complexity is defined by the number of data transmissions required to complete a single positioning operation. It shows that our TDOA-MCM has the highest accuracy but lowest transmission count among the mechanisms with clock correction.

Table 1. Comparison with existing positioning

Ref	Method	Implementation	Test Area	Synchronization	Complexity	Errors (cm)
[33]	TDOA/SDS-TWR	Simulation	9m one-way distance measurement	Synchronized	6	<25
[34]	EDTDOA	Experiment	16m×5.6m	Clock correction	Far greater than 9	<30
[21]	UWB-TDOA	Experiment	5m×6m	Clock correction	8	<15
[17]	A-TDOA	Experiment	6m×6m	Clock correction	9	<15
[31]	F-AltDS-TWR	Experiment	12m×12m	Clock correction	9	<11

Ours	TDOA-MCM	Simulation	10m×10m	Clock correction	5	<6
Ours	TDOA-MCM	Experiment	6m×8m	Clock correction	7	<10

5. Conclusion

The ideal clock-synchronized TDOA provides superior accuracy for UWB-based indoor positioning. However, clock drift or desynchronization can greatly reduce the positioning performance. This paper proposes a TDOA-based multi-path communication mechanism, TDOA-MCM, to address this challenge. We use one base station as the signal transmitter, and the signal arrives at the tag via both direct path and multi-path. Calculating the time difference between the two paths, there is no need for clock synchronization between the base stations and the tag. The performance is analyzed by the Cramer-Rao bound. It was demonstrated that each additional communication for clock compensation aggravated the effects of noise compared to the ideal TDOA. The proposed TDOA-MCM only adds one path between the stations (irrelevant to the tag), achieving positioning errors of less than 10 cm in real indoor experiments. Multiple tags are allowed in one positioning system as they do not transmit signals, and the passive mechanism can also protect the privacy of tag users.

In future research, we will incorporate machine learning methods to compensate for the clock drift and optimize the system for better accuracy. We will also consider improving positioning accuracy from other aspects, such as non-line-of-sight conditions, and hardware temperature compensation.

Acknowledgment

This work is supported by the Fundamental Research Program of Shanxi Province (No. 202203021222016).

References

[1] J. Ma, S. Feng, X. Li, X. Zhang and D. Zhang, “Research on the Internet of Things Architecture for Intelligent Passenger Transportation Services and its Application,” in *Proc. of the 2019 4th International Conference on Electromechanical Control Technology and Transportation (ICECTT)*, pp.194-197, 2019. Article (CrossRef Link)

[2] C. Wang, A. Xu, J. Kuang, X. Sui, Y. Hao and X. Niu, “A High-Accuracy Indoor Localization System and Applications Based on Tightly Coupled UWB/INS/Floor Map Integration,” *IEEE Sensors Journal*, vol.21, no.16, pp.18166-18177, Aug. 2021. Article (CrossRef Link)

[3] L. Barbieri, M. Brambilla, A. Trabattoni, S. Mervic and M. Nicoli, “UWB Localization in a Smart Factory: Augmentation Methods and Experimental Assessment,” *IEEE Transactions on Instrumentation and Measurement*, vol.70, pp.1-18, 2021. Article (CrossRef Link)

[4] J. Fu, Y. Fu and D. Xu, “Application of an Adaptive UKF in UWB Indoor Positioning,” in *Proc. of the 2019 Chinese Automation Congress (CAC)*, pp.544-549, 2019. Article (CrossRef Link)

[5] L. Qinghua, L. Sicheng, Y. Yipeng, J. Chunyu and Y. Xiaozhen, “An accurate maximum likelihood location method based on UWB platform,” in *Proc. of the 2019 14th IEEE International Conference on Electronic Measurement & Instruments (ICEMI)*, pp.515-521, 2019. Article (CrossRef Link)

[6] I. H. Brahmi, G. Abbruzzo, M. Walsh, H. Sedjelmaci and B. O'Flynn, "A fuzzy logic approach for improving the tracking accuracy in indoor localisation applications," in *Proc. of the 2018 Wireless Days (WD)*, pp.137-144, 2018. Article (CrossRef Link)
[7] G. T. Lee, S. B. Seo and W. S. Jeon, "Indoor Localization by Kalman Filter based Combining of UWB-Positioning and PDR," in *Proc. of the 2021 IEEE 18th Annual Consumer Communications & Networking Conference (CCNC)*, pp.1-6, 2021. Article (CrossRef Link)
[8] Y. Wang and K. C. Ho, "An Asymptotically Efficient Estimator in Closed-Form for 3-D AOA Localization Using a Sensor Network," *IEEE Transactions on Wireless Communications*, vol.14, no.12, pp.6524-6535, Dec. 2015. Article (CrossRef Link)
[9] N. Patwari, J.N. Ash, S. Kyperountas, A.O. Hero, R.L. Moses and N.S. Correal, "Locating the nodes: cooperative localization in wireless sensor networks," *IEEE Signal Processing Magazine*, vol.22, no.4, pp.54-69, Jul. 2005. Article (CrossRef Link)
[10] R. W. Ouyang, A. K.-S. Wong and C.-T. Lea, "Received Signal Strength-Based Wireless Localization via Semidefinite Programming: Noncooperative and Cooperative Schemes," *IEEE Transactions on Vehicular Technology*, vol.59, no.3, pp.1307-1318, Mar. 2010. Article (CrossRef Link)
[11] M. Zaidi, I. Bouazzi, M. I. Al-Rayif, M. Z. M. Shamim, M. Usman, "Low power hardware design and its mathematical modeling for fast-exact geolocalization system in wireless networks," *International Journal of Communication Systems*, vol.35, no.9, 2022. Article (CrossRef Link)
[12] J. He, Y. Geng and K. Pahlavan, "Toward Accurate Human Tracking: Modeling Time-of-Arrival for Wireless Wearable Sensors in Multipath Environment," *IEEE Sensors Journal*, vol.14, no.11, pp.3996-4006, Nov. 2014. Article (CrossRef Link)
[13] M. Zaidi et al., "Cooperative Scheme ToA-RSSI and Variable Anchor Positions for Sensors Localization in 2D Environments," *Complexity*, vol.2022, pp.1-11, 2022. Article (CrossRef Link)
[14] M. Qian et al., "An Overview of Ultra-Wideband Technology and Performance Analysis of UWB-TWR in Simulation and Real Environment," in *Proc. of the International Conference on Indoor Positioning and Indoor Navigation (IPIN)*, 2022. Article (CrossRef Link)
[15] K.C. Ho and Y.T. Chan, "Solution and performance analysis of geolocation by TDOA," *IEEE Transactions on Aerospace and Electronic Systems*, vol.29, no.4, pp.1311-1322, Oct. 1993. Article (CrossRef Link)
[16] Y. Zhou, C. L. Law, Y. L. Guan and F. Chin, "Indoor Elliptical Localization Based on Asynchronous UWB Range Measurement," *IEEE Transactions on Instrumentation and Measurement*, vol.60, no.1, pp.248-257, Jan. 2011. Article (CrossRef Link)
[17] S. He and X. Dong, "High-Accuracy Localization Platform Using Asynchronous Time Difference of Arrival Technology," *IEEE Transactions on Instrumentation and Measurement*, vol.66, no.7, pp.1728-1742, Jul. 2017. Article (CrossRef Link)
[18] B. Xu, G. Sun, R. Yu and Z. Yang, "High-Accuracy TDOA-Based Localization without Time Synchronization," *IEEE Transactions on Parallel and Distributed Systems*, vol.24, no.8, pp.1567-1576, Aug. 2013. Article (CrossRef Link)
[19] Y. Xue, W. Su, H. Wang, D. Yang and J. Ma, "A Model on Indoor Localization System Based on the Time Difference Without Synchronization," *IEEE Access*, vol.6, pp.34179-34189, 2018. Article (CrossRef Link)
[20] X. S. Chen et al., "Research on differential UWB indoor positioning system based on TDOA algorithm," *Modern Electronics Technique*, vol.41, no.6, pp.45-49, 2018. Article (CrossRef Link)
[21] J. Leng, and G. Ma, "Research on indoor robot TDOA asynchronous no reference ranging location method," *Electronic Measurement Technology*, vol.45, no.2, pp.1-6, 2022. Article (CrossRef Link)
[22] C. Tu et al., "Parameterized TDOA: Instantaneous TDOA Estimation and Localization for Mobile Targets in a Time-Division Broadcast Positioning System," *arXiv preprint arXiv:2410.23695*, 2024. Article (CrossRef Link)
[23] G. Xiao, Q. Dong, G. Liao, S. Li, K. Xu, and Y. Quan, "High-Precision Joint TDOA and FDOA Location System," *Remote Sensing*, vol.16, no.4, 2024. Article (CrossRef Link)

[24] A. Kirmaz, T. Şahin, D. S. Michalopoulos and W. Gerstacker, "ToA and TDoA Estimation Using Artificial Neural Networks for High-Accuracy Ranging," *IEEE Journal on Selected Areas in Communications*, vol.41, no.12, pp.3816-3830, Dec. 2023. Article (CrossRef Link)
[25] S. Maranò, W. M. Gifford, H. Wymeersch and M. Z. Win, "NLOS identification and mitigation for localization based on UWB experimental data," *IEEE Journal on Selected Areas in Communications*, vol.28, no.7, pp.1026-1035, Sept. 2010. Article (CrossRef Link)
[26] G. Zhang, Z. Deng, L. Wen, L. Ge, H. Ke and J. Jiao, "An UWB location algorithm for indoor NLOS environment," in *Proc. of the 2018 Ubiquitous Positioning, Indoor Navigation and Location-Based Services (UPINLBS)*, pp.1-6, 2018. Article (CrossRef Link)
[27] Y. Cheng and T. Zhou, "UWB Indoor Positioning Algorithm Based on TDOA Technology," in *Proc. of the 2019 10th International Conference on Information Technology in Medicine and Education (ITME)*, pp.777-782, 2019. Article (CrossRef Link)
[28] I. Sharp, K. Yu and Y. J. Guo, "GDOP Analysis for Positioning System Design," *IEEE Transactions on Vehicular Technology*, vol.58, no.7, pp.3371-3382, Sept. 2009. Article (CrossRef Link)
[29] A. Antoniou, and W.-S. Lu, Practical Optimization: Algorithms and Engineering Applications, Texts in Computer Science, New York: Springer, 2021. Article (CrossRef Link)
[30] S. K. Sengijpta, "Fundamentals of Statistical Signal Processing: Estimation Theory," *Technometrics*, vol.37, no.4, pp.465-466, 1995. Article (CrossRef Link)
[31] J. Zhang, W. Wang, X. She and X. Li, "2-D Indoor Passive Real-Time Location System Based on Ultrawideband Technology," *IEEE Transactions on Instrumentation and Measurement*, vol.71, pp.1-17, 2022. Article (CrossRef Link)
[32] J. Sidorenko, V. Schatz, N. Scherer-Negenborn, M. Arens and U. Hugentobler, "DecaWave Ultra-Wideband Warm-Up Error Correction," *IEEE Transactions on Aerospace and Electronic Systems*, vol.57, no.1, pp.751-760, Feb. 2021. Article (CrossRef Link)
[33] Q. Yin, H. Yu, "TDOA/SDS-TWR combined ranging method based on ultra-wideband," *Electronic Measurement Technology*, vol.44, no.4, pp.75-79, 2021. Article (CrossRef Link)
[34] A. Vashistha and C. L. Law, "A Novel E-DTDOA Based One-Way Ranging Using UWB-IR With Unsynchronized Anchors," *IEEE Transactions on Industrial Informatics*, vol.17, no.2, pp.1274-1286, Feb. 2021. Article (CrossRef Link)



Xuan Lu received the B.S. and Ph.D. degrees from Nanjing University of Science and Technology, in 2008 and 2016, respectively. She is currently an associate professor with the College of Physics and Electronic Engineering at Shanxi University. Her current research interests include radar detection and ultra-wideband techniques.



Jinhong Guo received the B.S. degree from the School of Physical and Electronic Engineering at Shanxi University, Taiyuan, China, in 2022, and is currently pursuing the M.S. degree at the same university. His research interests are in UWB indoor positioning.



Furong Peng received his Ph.D. degree from Nanjing University of Science and Technology, Nanjing, China, in 2017. He is currently an Associate Professor at the Institute of Big Data Science and Industry, Shanxi University, Taiyuan, China. His research interests include recommendation system and data mining.



Yu Dong received the B.S degree and M.S degree in College of Physics And Electronic Engineering from Shanxi University, Taiyuan, China, in 2019 and 2023, and she is currently studying for a Ph.D degree with the College of Computer Science and Electronic Engineering, Hunan University, Changsha, China. Her current research interests are the circuit design and applications of optimization problem solving based on memristors.